THE JOURNAL OF BIOLOGICAL CHEMISTRY VOL. 292, NO. 7, pp. 2992–3004, February 17, 2017

Peptide from Sea Anemone *Metridium senile* Affects Transient Receptor Potential Ankyrin-repeat 1 (TRPA1) Function and Produces Analgesic Effect*

Received for publication, September 6, 2016, and in revised form, January 3, 2017 Published, JBC Papers in Press, January 11, 2017, DOI 10.1074/jbc.M116.757369

Yulia A. Logashina[‡§], Irina V. Mosharova[‡], Yulia V. Korolkova[‡], Irina V. Shelukhina[‡], Igor A. Dyachenko[¶], Victor A. Palikov[¶], Yulia A. Palikova[¶], Arkadii N. Murashev[¶], Sergey A. Kozlov[‡], Klara Stensvåg[‖], and Yaroslav A. Andreev[‡§1]

From the [‡]Shemyakin-Ovchinnikov Institute of Bioorganic Chemistry, Russian Academy of Sciences, ul. Miklukho-Maklaya 16/10,117997 Moscow, Russia, the [§]Sechenov First Moscow State Medical University, Institute of Molecular Medicine, Trubetskaya St. 8, Bldg. 2, 119991 Moscow, Russia, the [¶]Branch of the Shemyakin-Ovchinnikov Institute of Bioorganic Chemistry, Russian Academy of Sciences, 6 Nauki Avenue, 142290 Pushchino, Moscow, Russia, and the [‖]Norwegian College of Fishery Science, University of Tromsø, N9037 Tromsø, Norway

Edited by Paul E. Fraser

The transient receptor potential ankyrin-repeat 1 (TRPA1) is an important player in pain and inflammatory pathways. It is a promising target for novel drug development for the treatment of a number of pathological states. A novel peptide producing a significant potentiating effect on allyl isothiocyanate- and diclofenac-induced currents of TRPA1 was isolated from the venom of sea anemone *Metridium senile*. It is a 35-amino acid peptide cross-linked by two disulfide bridges named τ-AnmTX Ms 9a-1 (short name Ms 9a-1) according to a structure similar to other sea anemone peptides belonging to structural group 9a. The structures of the two genes encoding the different precursor proteins of Ms 9a-1 were determined. Peptide Ms 9a-1 acted as a positive modulator of TRPA1 *in vitro* but did not cause pain or thermal hyperalgesia when injected into the hind paw of mice. Intravenous injection of Ms 9a-1 (0.3 mg/kg) produced a significant decrease in the nociceptive and inflammatory response to allyl isothiocyanate (the agonist of TRPA1) and reversed CFA (Complete Freund's Adjuvant)-induced inflammation and thermal hyperalgesia. Taken together these data support the hypothesis that Ms 9a-1 potentiates the response of TRPA1 to endogenous agonists followed by persistent functional loss of TRPA1-expressing neurons. We can conclude that TRPA1 potentiating may be useful as a therapeutic approach as Ms 9a-1 produces significant analgesic and anti-inflammatory effects in mice models of pain.

Transient receptor potential ankyrin-repeat 1 (TRPA1)[2] receptors play a significant role in initiation and development of neurogenic inflammatory pain. TRPA1 consists of four identical subunits that form a transmembrane channel. Each subunit contains six transmembrane domains and has a long cytoplasmic N terminus that comprises many ankyrin repeats (16 in humans; 14–17 in mice) (1). Ankyrin repeats are 33-amino acid motifs found within many proteins that mediate protein-protein interactions. TRPA1 receptors are expressed in mammalian somatic and visceral sensory neurons that innervate skin, lung, or intestinal epithelium, pancreas cells, and mucosa of the oral cavity. TRPA1 receptors co-localize with transient receptor potential vanilloid 1 (TRPV1) in a subset of small diameter, unmyelinated, peptidergic neurons. TRPA1 is calcium-permeable cation channel activated by exogenous and endogenous irritants and mechanical stimuli. Several different ways for the activation of TRPA1 have been found. Most of the known electrophilic agonists act via covalent modification of cysteine residues at the N terminus of the TRPA1 receptor. Non-electrophilic substances such as some NSAIDs, Δ^9-tetrahydrocannabinol, and 2-aminoethoxydiphenyl borate can activate TRPA1 via reversible binding (2–4).

Electrophilic TRPA1 agonists from cigarette smoke such as α,β-aldehydes (acrolein, crotonaldehyde) trigger eye irritation, cough, and neurogenic inflammation of the airways (5). Substances from food that target TRPA1 are the pungent compounds of mustard (allyl isothiocyanate (AITC); Ref. 6), cinnamon (cinnamaldehyde; Refs. 7, 8), and garlic (allicin; Ref. 9). Industrial emissions also contain TRPA1 activators such as toluene diisocyanate (10), zinc (11), hypochlorite, and hydrogen peroxide (12). General anesthetics like desflurane (13) and isoflurane (14) can stimulate bronchial contraction via activation of TRPA1 and therefore cause significant side effects.

Endogenous agonists of TRPA1 are compounds generated during tissue inflammation, asthma, chemical hypersensitivity, chronic cough, and chronic obstructive pulmonary dis-

* This work was supported by Russian Science Foundation Grant 16-15-00167, the Functional Genomics (FUGE) programme, and the Biotek 2021 programme of the Research Council of Norway, project XBioPepS (Grant 208546). The authors declare that they have no conflicts of interest with the contents of this article.

This work is dedicated to Professor Eugene V. Grishin and his untimely death.

Nucleotide sequences reported in this paper have been submitted to the European Nucleotide Archive with accession numbers LT577947 and LT577948. Peptide τ-AnmTX Ms 9a-1 has been submitted to Uniprot with submission number C0HK13.

[1] To whom correspondence should be addressed. Tel.: 7495-336-40-22; Fax: 7495-330-7301; E-mail: ay@land.ru.

[2] The abbreviations used are: TRPA1, transient receptor potential ankyrin 1; TRPV1, transient receptor potential vanilloid 1; Ms 9a-1, τ-AnmTX Ms 9a-1; ACN, acetonitrile; AITC, allyl isothiocyanate; CFA, complete Freund's adjuvant; NAPQI, *N*-acetyl-*p*-benzoquinoneimine; p-BQ, *p*-benzoquinone; NSAID, nonsteroidal anti-inflammatory drug; RACE, rapid amplification of cDNA ends; Ugr, *U. grebelnyi*; Ms, *M. senile*; DRG, dorsal root ganglion; p.o., per os.

ease. These are 4-hydroxynonenal (15), 4-oxononenal (16), nitrooleic acid (10), and the prostaglandin derivative 15-deoxy-Δ(12,14)-prostaglandin J2 (15–18). Thus, TRPA1 is an important target for the design of novel analgesic and anti-inflammatory drugs.

Venomous animals produce different polypeptides for hunting and defense. Venom compounds interact with diverse biological targets, producing different effects that could be used in scientific research and in pharmacology (19, 20). Such multitasking of venom is provided by the generation of large families of polypeptide molecules, each of them being highly specific to a certain receptor. Venoms of sea anemones have already become a source for characterization of several polypeptides with intriguing properties such as the $Kv_{1.3}$ blocker (21), ASIC3 inhibitors (22–24), TRPV1 modulators (25, 26), and many others (20).

In this paper we describe the isolation and characterization of novel peptide τ-AnmTX Ms 9a-1 (short name Ms 9a-1) from the venom of sea anemone *Metridium senile*. Ms 9a-1 is a 35-residue peptide containing four cysteines that is structurally similar to the β-hairpin ASIC3 inhibitor Ugr 9a-1 previously isolated from the venom of the sea anemone *Urticina grebelnyi* (23). Peptide Ms 9a-1 enhances the response of the TRPA1 receptor to agonists *in vitro* and produces significant antinociception and anti-inflammatory effects when injected into mice.

Results

Peptide Isolation and Primary Structure Determination—The crude peptide fraction of *M. senile* venom produced a potentiating effect on agonist-activated rTRPA1 response in fluorescent inflow calcium assay on stable CHO cell lines expressing the receptor. The active compound was isolated in two reverse-phase HPLC separation steps with fractions activity testing (Fig. 1). The average molecular weight of the active peptide was estimated by matrix-assisted laser desorption ionization (MALDI) mass spectrometry and was equal to 3654.4 Da.

The N-terminal sequence of 34 amino acid residues was established by Edman degradation. The C-terminal residue was predicted as Ser by the difference between calculated molecular weight of the sequenced fragment and molecular weight of peptide measured by MALDI. The primary structure was confirmed by analysis of cDNAs coding for the peptide that were obtained by the 3′- and 5′-rapid amplification of cDNA ends (RACE) method. In 3′-RACE the PCR product (~250 bp) was obtained using total RNA from *M. senile* as a template, the two degenerated primers MS-d1 and MS-d2, and the universal primer T7Cap. The DNA fragment coding for the signal peptide and 5′-untranslated region was amplified by using the 5′-RACE technique with the reverse primers MS-r1 and MS-r2 and the universal primer T7Cap. A full precursor sequence was produced using primers MS-5′-end and MS-3′-end. Clones' sequencing revealed two genes (named *ms9.1* and *ms9.2*) coding for precursor proteins MS9.1 and MS9.2 containing the target peptide (Fig. 2, *A* and *B*). The calculated average molecular mass 3654.4 Da was equal to the measured molecular mass for the native peptide.

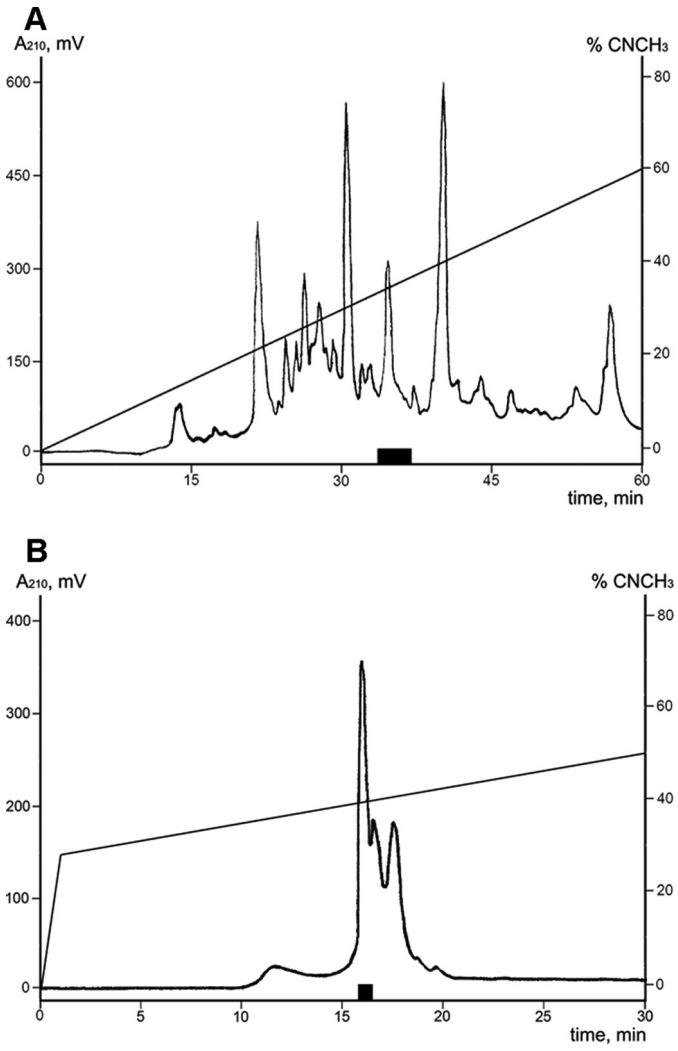

FIGURE 1. **Isolation of the active peptide from the *M. senile* venom.** *A*, HPLC separation of the crude peptide fraction on a reverse-phase column Jupiter C5 (250 × 10 mm) using a linear gradient of ACN concentration (0–60% in 60 min) in 0.1% TFA and a flow rate of 5 ml/min. *B*, HPLC of active fraction on a Synergi Fusion-RP column (250 × 3 mm) using a gradient of ACN concentration (0–30% for 1 min, 30–50% for 30 min) in the presence of 0.1% TFA and a flow rate of 0.5 ml/min. Fractions exercised a potentiating activity on rTRPA1 are marked with a *black box*.

Precursor proteins consist of similar signal peptides, spacer regions, and active peptide and differ in several substitutions in the C-terminal region coding for close structural homologs of the active peptide (Fig. 2*B*). The 35-residue-long active peptide is located next to the spacer region after the signal peptide sequence. The cysteine distribution pattern of the mature sequence (Fig. 2*C*) was similar to sea anemone peptides of group 9a, so in accordance with a convenient nomenclature (27) the peptide was named τ-AnmTX Ms 9a-1 (short name Ms 9a-1). C-terminal homological peptides from precursors Ms9.1 and Ms9.2 were named AnmTX Ms 9a-2 (Ms 9a-2) and AnmTX Ms 9a-3 (Ms 9a-3), respectively. Peptides Ms 9a-1, Ms 9a-2, and Ms 9a-3 were flanked by processing site sequence DP (EP) (Fig. 2, *A* and *B*). Such maturation sequences can be removed by dipeptidyl peptidases and are usual for sea anemone, hymenoptera, and amphibian toxins (28). There were no attempts at identification, isolation, or characterization of Ms

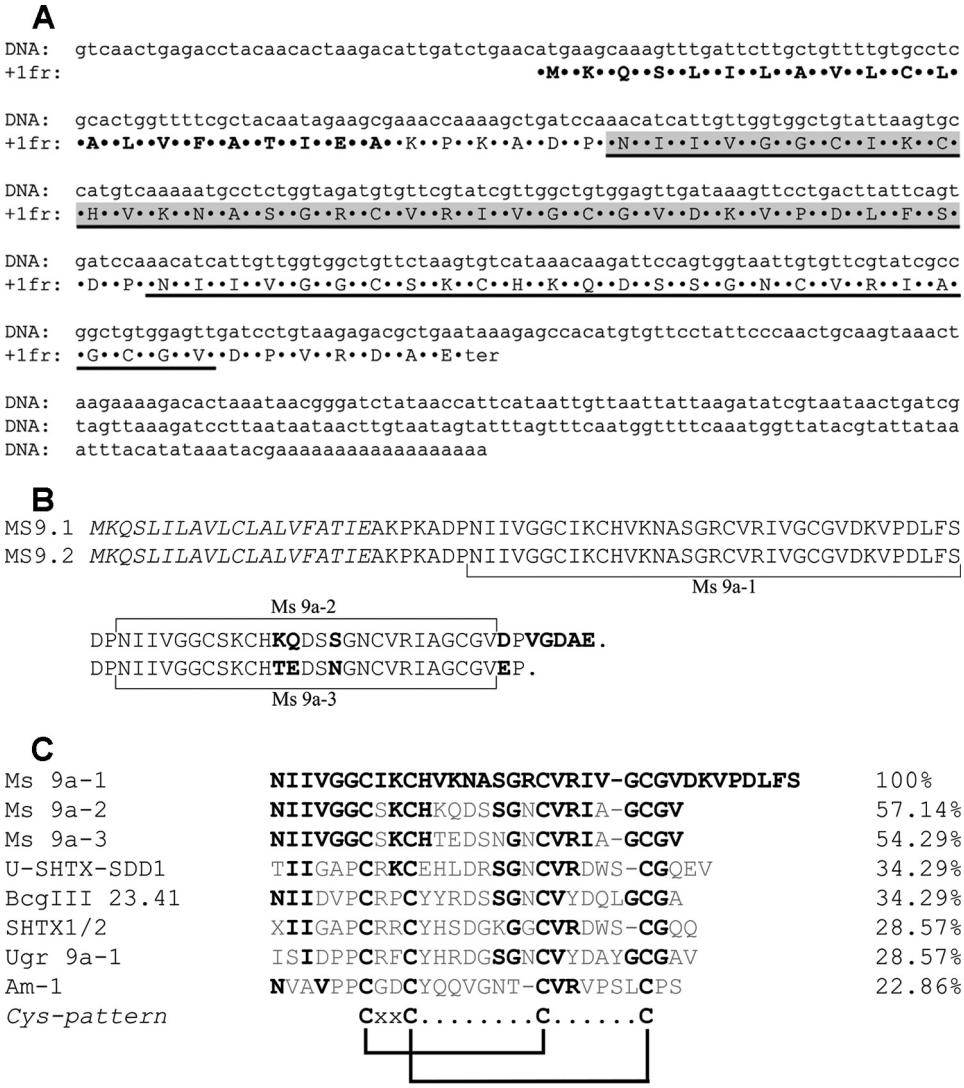

FIGURE 2. **Structural organization of precursor proteins.** *A*, nucleotide sequence of *ms9.1* cDNA accompanied by deduced amino acid sequence. The signal peptide sequence is marked in *bold*, determined mature peptide sequences are *underlined*, and the Ms 9a-1 peptide is highlighted in *gray*. *B*, alignment of protein sequences of Ms 9a-1 precursors deduced from *ms9.1* and *ms9.2* genes. The signal peptide sequences are shown in *italics*, and different amino acids are in *bold*. *C*, multiple sequence alignment for three novel peptides from *M. senile* and other sea anemone toxins from structural class 9a: peptide U-SHTX-Sdd11 (C0HJB4) from *Homostichanthus duerdeni*; SHTXI/2 (P0C7W7) from *Stichodactyla haddoni*; Bcg III 23.41 toxin (P86466) from *Bunodosoma cangicum*; Am-1 (P69929) from *Antheopsis maculata*; Ugr 9a-1 (S4S1V7) from *U. grebelnyi*. Residues identical to the Ms 9a-1 sequence are *highlighted*. The cysteine distribution pattern for structural class 9a is *shown at the bottom*.

9a-2 and Ms 9a-3 peptides as they were out of the scope of this study.

Primary Structure Homology—A BLAST search revealed the homology of the Ms 9a-1 structure to sea anemone peptides U-SHTX-Sdd1 (29), Bcg-III-23.41 (30), and SHTX-1/SHTX-2 (31) (Fig. 2*C*). These peptides, with two disulfide bridges, belong to class 9a of sea anemone peptides with a boundless β-hairpin fold, as was established for peptide Ugr 9a-1, isolated from the venom of sea anemone *U. grebelnyi* (23). All of the previously found peptides differ in their cellular target. Bcg-III-23.41 and SHTX-1/SHTX-2 were found to be weak voltage-gated potassium channel blockers (30, 31). Ugr 9a-1 was characterized as the inhibitor of ASIC3 channels, producing significant analgesic activity (23). U-SHTX-Sdd1, known as the first sea anemone toxin with O-HexNAc-threonine posttranslational modification at position 1, has not been characterized by target yet (29). These peptides target other biological functions and do not have significant primary structure similarity to Ms9a-1 (max 34% of identity). The most homologous peptides are Ms 9a-2 and Ms 9a-3, predicted from the same protein precursors. The main features that distinguish Ms 9a-1 from Ms 9a-2 and Ms 9a-3 are a long C-terminal tail and a nonhomological region between 2 and 3 Cys residues (Fig. 2*C*). Presumably, these nonhomologous residues can be, at least partially, responsible for peptide recognition of TRPA1.

Recombinant Polypeptide Production—To provide a sufficient amount of peptide for functional investigations, recombinant Ms 9a-1 was produced as the fusion protein with thioredoxin in the prokaryotic expression system. Thioredoxin ensures high yields of cysteine-containing polypeptides with native conformation (23, 32, 33). A synthetic gene coding for the mature peptide Ms 9a-1 was constructed and cloned into expression vector pET32b(+). The construction of pET32b+Ms 9a-1 was used to transform *Escherichia coli*

BL21(DE3) cells. The fusion protein was isolated by metal affinity chromatography and cleaved by CNBr to release the recombinant peptide. Recombinant Ms 9a-1 was purified by reverse-phase HPLC. The final yield of the target peptide was estimated to be ~2.4 mg/liter of the cell culture. The recombinant peptide had the same molecular weight and amino acid sequence of five N-terminal residues as the natural Ms 9a-1. Retention time during the co-injection of both peptides on a reverse-phase column was also identical, verifying the proper folding of the recombinant Ms 9a-1.

Ms 9a-1-potentiated Response of CHO-rTRPA1 Cells to AITC—Ms 9a-1 activity was measured by fluorescent influx calcium assay on CHO-rTRPA1 cells. The Ca^{2+} response was induced by adding AITC. The crude peptide fraction of *M. senile* venom potentiates the response to 100 μM AITC up to 30%. Native peptide Ms 9a-1 showed the same potentiating activity in a relevant concentration (Fig. 3*A*). Recombinant and native peptides showed the same activity in equal concentration. Neither the native nor the recombinant peptide caused Ca^{2+} influx in rTRPA1-CHO cells alone.

Preliminary experiments revealed that the efficacy of potentiation depended on the TRPA1 activation level. Analysis of dependence for the potentiating effect of Ms 9a-1 revealed the significant impact of agonist concentration (AITC). AITC produced the dose-dependent increase of $[Ca^{2+}]_i$ response in the concentration range 15–500 μM, whereas 1000 μM AITC produced less response than 500 μM, most probably due to TRPA1 agonist-induced desensitization. Preincubation with Ms 9a-1 (1 μM) did not cause significant changes in response at low (15–50 μM) or high (500–1000 μM) AITC concentrations. The maximal potentiating action of Ms 9a-1 (35–55%) was observed at agonist concentrations producing the middle range of $[Ca^{2+}]_i$ responses (100–300 μM) (Fig. 3*B*).

Electrophysiology—Ms 9a-1 produced a significant concentration-dependent potentiating effect on diclofenac activation of rTRPA1 expressed in *Xenopus laevis* oocytes (Fig. 4). Recordings in repeated voltage ramp pulses from −80 mV to +80 mV showed the significant potentiating effect on the inward current of TRPA1, but this effect was not stable on the outward current (Fig. 4*A*). The maximal effect reached ~90% for potentiation of diclofenac-induced inward currents at a peptide concentration >1 μM (Fig. 4*B*). The EC_{50} of Ms 9a-1 for the inward current potentiation at −80 mV was 122 ± 41 nM (n_H 0.79 ± 0.19). A stable potentiating effect of the peptide on the outward current was achieved by the second protocol utilized, repeating voltage steps from −20 to +80 mV (Fig. 5). The maximal observed potentiating effect reached ~80% at a peptide concentration >1 μM when diclofenac or AITC was used as the activation stimuli (Fig. 5, *A* and *D*). The calculated EC_{50} of Ms 9a-1 at diclofenac activation was 30 ± 8.6 nM, with n_H 0.62 ± 0.15 (Fig. 5*B*). Therefore, the efficacy of the peptide to potentiate inward and outward currents is different. Ms9a-1 more efficiently potentiated outward currents of TRPA1 at low concentrations but equally affected both currents at concentrations >300 nM. The peptide did not cause measurable desensitization of TRPA1 receptors upon repeated stimulation by diclofenac in the presence of Ms 9a-1, the only strong potentiating effect observed (Fig. 5*C*).

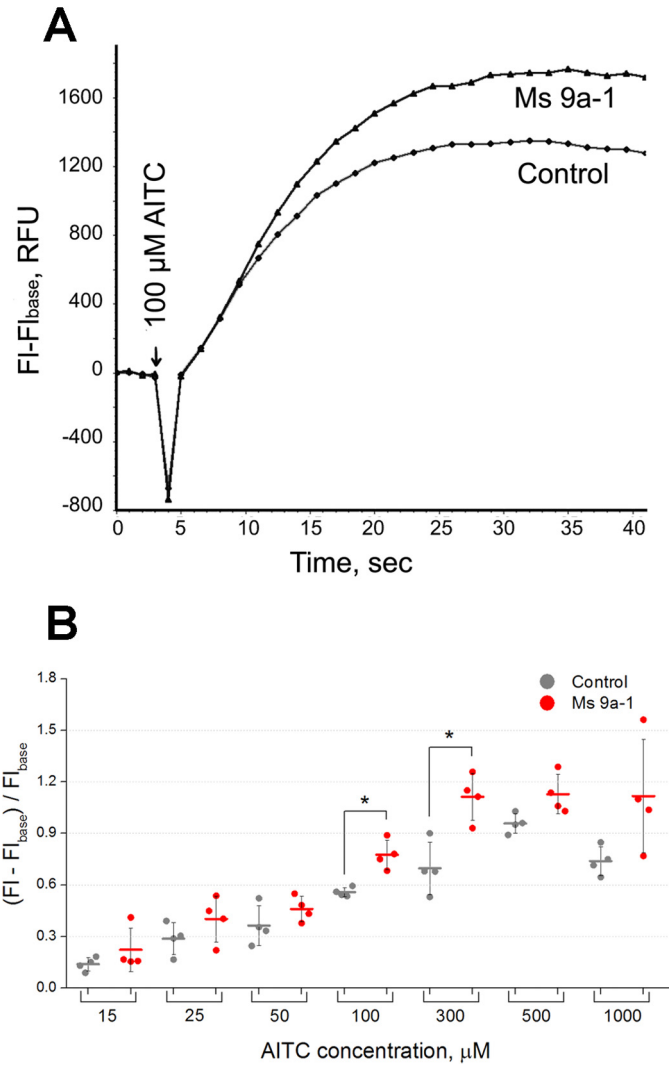

FIGURE 3. **Potentiating effect of Ms 9a-1 on rTRPA1.** *A*, $[Ca^{2+}]_i$ responses of rTRPA1-CHO cells to 100 μM AITC in buffer only and in the presence of native Ms 9a-1 (500 nM). The data shown are representative average plots ($n = 4$) of the fluorescence signals during assays. $[Ca^{2+}]_i$ responses were measured as changes in fluorescence intensity before (Fl_{base}) and after agonist addition (Fl). *B*, variable potentiating efficacy of recombinant Ms 9a-1 (1 μM) with different (15–1000 μM) concentrations of AITC. Data are expressed as the mean ± S.D. ($n = 4$); *, $p < 0.05$ (two-tailed *t* test). *RFU*, relative fluorescence units.

We next used cultured dorsal root ganglion (DRG) neurons to study the potentiating effects of Ms9a-1 on $[Ca^{2+}]_i$ rise mediated by TRPA1 in sensory neurons. Ms9a-1 (300 nM) produced a significant increase of 157 ± 88% ($n = 30$) in calcium response of DRG neurons to AITC (Fig. 6, *A* and *D*), whereas application of buffer did not provoke the significant response of DRG neurons (Fig. 6, *B* and *D*). Application of MS9a-1 alone did not induce any response of cultured sensory neurons (Fig. 6*C*).

Additionally, peptide Ms 9a-1 was tested on several ion channels for inhibitory/potentiating effects and showed neither agonistic nor antagonistic activity on rTRPV1, hTRPV3, rASIC1a, or hASIC3 at a concentration of 3 μM (not shown).

In Vivo Experiments—Compounds that activate TRPA1 cause pain and neurogenic inflammation accompanied with thermal and mechanical hyperalgesia (34). Thus, we examined whether Ms 9a-1 could cause pain or thermal hyperalgesia. Nei-

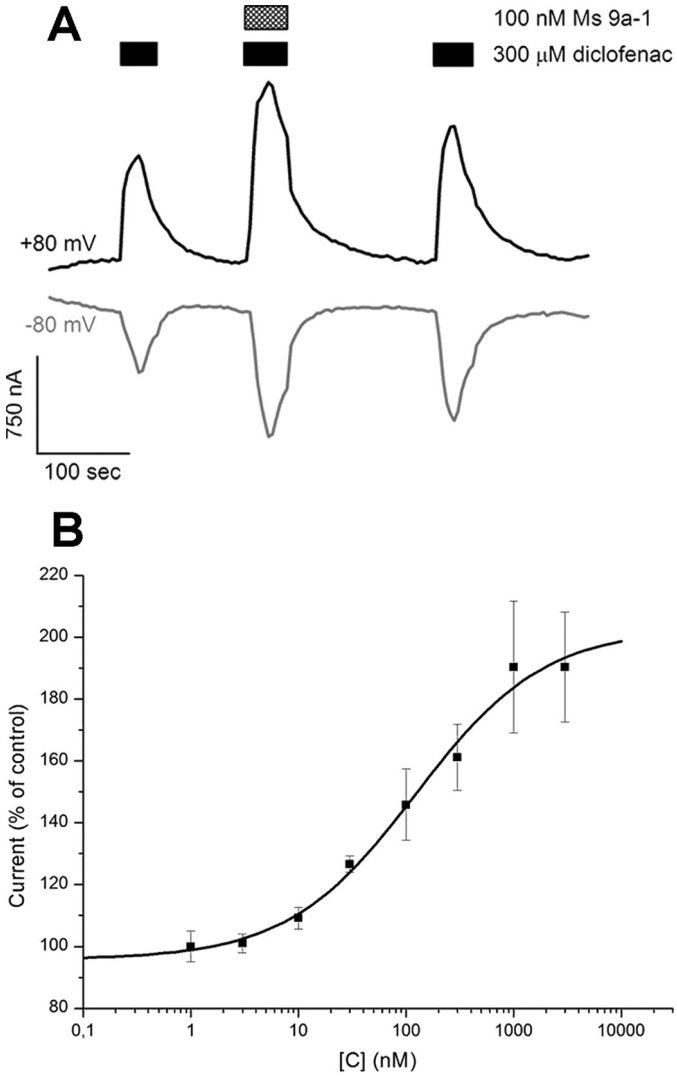

FIGURE 4. **Action of Ms 9a-1 on diclofenac-induced inward and outward TRPA1 currents.** *A*, representative trace of Ms 9a-1 effect on whole-cell currents through *X. laevis* oocytes expressing rTRPA1. The currents were evoked by 300 μM diclofenac and were recorded at +80 (*black*) and −80 mV (*gray*). *B*, dose-response curve of Ms 9a-1 action on diclofenac-induced inward TRPA1 current. Each point is the mean ± S.E. of 4–7 measurements. Data were fitted by the logistic equation.

ther pain response within 15 min after intraplantar injection of 2.5 μg of Ms 9a-1 nor thermal hyperalgesia 2 h after injection was observed (not shown).

Because Ms 9a-1 significantly potentiates the response to AITC *in vitro*, we tested whether the peptide could modulate response to this TRPA1 agonist in mice. The dosage of AITC (10 μl, 0.5% in saline) was chosen to provoke a nearly half-maximal response to AITC in licking and guarding. Administration of AITC (10 μl, 0.5% in saline) into the plantar surface of the hind paw induced licking and guarding of this paw together with swelling of the paw due to neurogenic inflammation, as described previously (35). Intravenous administration of Ms 9a-1 (0.3 mg/kg) 30 min before agonist injection significantly reduced AITC-induced nocifensive behavior, decreasing the duration of paw guarding (~78%) (Fig. 7*A*) and the number of paw licks (~55%) (Fig. 7*B*). Ms 9a-1 also significantly reduced the development of neurogenic inflammation, decreasing paw edema by ~42 and ~50% compared with the control 2 and 4 h after AITC injection, respectively (Fig. 7*C*). No significant effect of Ms 9a-1 was observed at a dose of 0.03 mg/kg (not shown).

Complete Freund's Adjuvant (CFA)-induced thermal hyperalgesia is a general model of inflammation. Injection of CFA into the hind paw produces swelling and increased sensitivity to noxious mechanical and thermal stimuli (hyperalgesia). Administration of Ms 9a-1 (0.3 mg/kg, intravenously (i.v.)) significantly reversed thermal hyperalgesia (~56% of reversal) within 30 min. Moreover, the peptide reduced development of paw edema by 32, 35, and 39% compared with the control 2, 4, and 24 h, respectively, after administration (Fig. 8, *A* and *B*). There was no significant effect of Ms 9a-1 observed at a dose of 0.03 mg/kg. Administration of selective TRPA1 antagonist A-967079 (20 mg/kg, p.o.) 1 h before the peptide completely blocked the effect of Ms 9a-1 (0.3 mg/kg, i.v.) on CFA-induced thermal hyperalgesia.

The TRPV1 (capsaicin receptor) is largely co-expressed with TRPA1 on sensory neurons. Intravenous administration of Ms9a-1 (0.3 mg/kg) 30 min before capsaicin injection significantly reduced pain-related behavior (~50% inhibition) (Fig. 8*D*).

No changes in locomotor activity in the open-field test were found after i.v. administration of 0.3 mg/kg Ms 9a-1. All basic parameters of locomotion tests, such as traveled distance, rearing, velocity, and time spent in the center and peripheral zones were the same for the control and Ms 9a-1 groups (not shown).

Discussion

TRPA1 is an extremely promising target for novel drug development for the treatment of a variety of pathological states associated with inflammation. This nonselective cation channel is mainly expressed in sensory neurons and activated by endogenous ligands produced during inflammation or oxidative stress as well as by exogenous electrophilic chemicals such as AITC, cinnamaldehyde, allicin, and acrolein (1–5) and some other chemicals such as menthol, NSAIDs, and general anesthetics. Additionally, TRPA1 can also be activated indirectly via phospholipase C (PLC) and PKC pathways (36). Activation of TRPA1 depolarizes the membrane of sensory neurons, initiating both a signal of pain or itch to the CNS and the release of proinflammatory peptides such as substance P and calcitonin gene-related peptide (CGRP), provoking the local inflammatory response. Thus, TRPA1 activators can induce neuropathic and inflammatory pain *in vivo* (17, 18). Moreover, a mutation in the gene coding for TRPA1 can cause autosomal-dominant pain syndrome (37). Normally TRPA1 is considered a chemosensor and also takes part in mechanosensitivity (38).

A few TRPA1 antagonists have been reported in the literature to date: AP-18 (39), A-967079 (40), HC-030031 (41), and GRC17536 (42). But a number of additional scaffold classes have also been described in patents (43). These are small molecule antagonists that display very promising *in vivo* activity in animal models of hypersensitivity and cold hyperalgesia, but effective doses are too high for drug development, except for GRC17536, which is in phase 2 clinical trials on diabetic neuropathy and respiratory disorders.

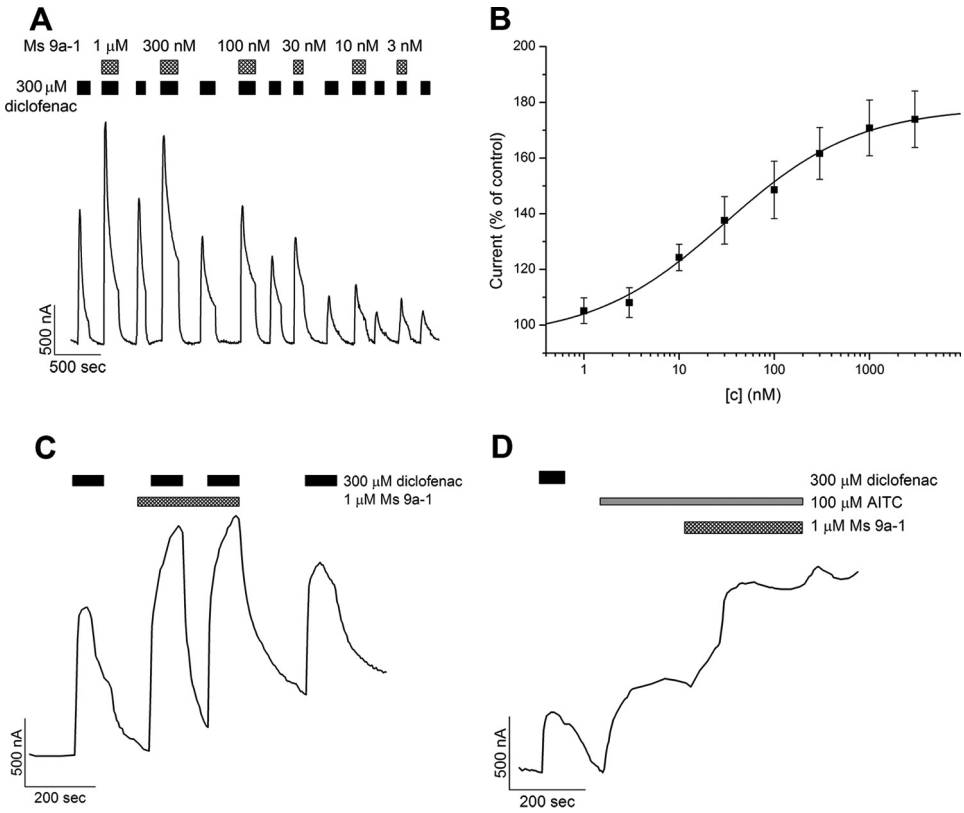

FIGURE 5. **Action of Ms 9a-1 on outward rTRPA1 current.** *A*, representative trace of Ms9a-1 effect on whole-cell current through rTRPA1 evoked by diclofenac at −20 to +80 mV step pulses. *B*, dose-response curve for the potentiating effect of Ms 9a-1 on diclofenac-induced TRPA1. Each point is the mean ± S.E. of 3–7 measurements. Data were fitted by the logistic equation. *C*, pre- and post incubation with Ms 9a-1 did not cause desensitization of the next diclofenac-induced TRPA1 response. *D*, representative trace of Ms 9a-1 potentiating effect on AITC-induced currents of TRPA1.

Although inhibition of TRPA1 seems the most logical treatment strategy to achieve pain relief in inflammatory and neuropathic diseases, it was shown that intraplantar, systemic, or spinal injection of some TRPA1 activators can also disrupt nociceptive signaling (3, 44–46). Consequently, the final outcome of TRPA1 activation crucially depended on the action spot and degree of TRPA1 activation. The analgesic effect of TRPA1 activation could contribute to the pharmacological action of some nonsteroidal anti-inflammatory drugs (acetaminophen, fenamates, and arylalkanoic acids) (2, 3) and extract of feverfew (46).

In this work a new sea anemone peptide, Ms 9a-1, was isolated from *M. senile* venom, providing evidence of a favorable outcome of TRPA1 potentiation on inflammatory pain development. To our knowledge Ms 9a-1 is the first peptide molecule that potentiates the TRPA1 receptor. No direct activation of TRPA1 by Ms 9a-1 was observed in either Ca^{2+} imaging testing or electrophysiological experiments. But when the peptide was co-applied with TRPA1 agonists (AITC or diclofenac), Ms 9a-1 increased receptor response. Ms 9a-1 did not act as a receptor agonist and did not cause pain or thermal hypersensitivity when it was injected into the hind paw of mice. But preadministration of Ms 9a-1 significantly reduced pain response to AITC (Fig. 7) and reversed CFA-induced thermal hyperalgesia and inflammation (Fig. 8). Thus, Ms 9a-1 administration *in vivo* significantly changes the inflammatory response.

Several research groups have reported analgesic properties of TRPA1 agonists to date. For example, some activators of TRPA1, such as *p*-benzoquinone (p-BQ) and *N*-acetyl-*p*-benzoquinoneimine (NAPQI), metabolites of acetaminophen, were found to be powerful analgesics (3). Metabolites of acetaminophen significantly activated TRPA1 *in vitro* in transfected HEK293 cells and rat DRG neurons but produced significant antinociceptive responses *in vivo* when administrated intrathecally. Activation of TRPA1 produced a depolarization block as well as an extensive and sustained inhibition of voltage-gated calcium and sodium currents in DRG neurons, which is considered to be a mechanism of spinal analgesia evoked by p-BQ and NAPQI.

A similar mechanism of action was found for a TRPA1 partial agonist, parthenolide, derived from feverfew (*Tanacetum parthenium*). This small electrophilic molecule is capable of activating TRPA1 in trigeminal neurons, and after initial stimulation it desensitizes the TRPA1 channel and decreases the ability of TRPA1-expressing nerve terminals to respond to any other stimuli. Notably, parthenolide induces nociceptive behavior and allodynia before response desensitization (46). Also, an interesting example is 15-deoxy-Δ(12,14)-prostaglandin J2, an endogenous electrophilic TRPA1 activator (47) that can produce an antinociceptive effect when injected into a mouse paw (45). Thus, the outcome of TRPA1 activation by agonists depends on their chemical properties, which predetermine the rate of TRPA1 desensitization and abilities of neurons to respond to other stimuli.

Taking into account these studies, the *in vivo* mechanism of antinociception produced by Ms 9a-1 could be proposed. Most

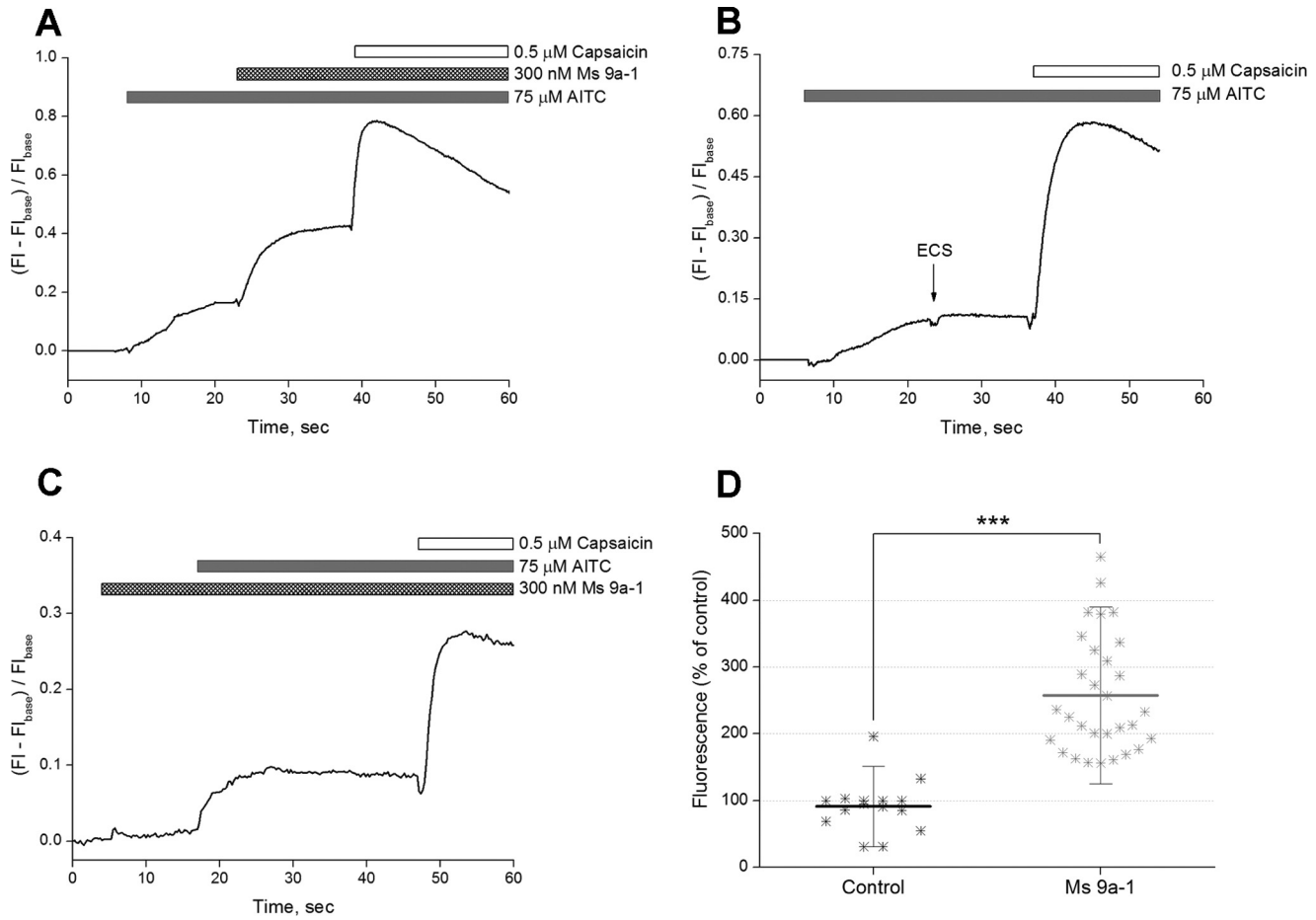

FIGURE 6. **Potentiating effect of Ms 9a-1 on AITC-induced $[Ca^{2+}]_i$ rise mediated by TRPA1 in rat-cultured DRG neurons.** Shown are representative traces. *A*, Ms 9a-1 (300 nM) increased cellular response to AITC. *B*, mock application of buffer solution (*ECS*) did not produce any significant response. C, Ms 9a-1 (300 nM) did not induce an increase in $[Ca^{2+}]_i$ of DRG neurons. $[Ca^{2+}]_i$ responses were measured as normalized changes in fluorescence intensity before (Fl_{base}) and after samples addition (*Fl*). *D*, pooled data: fluorescence (% of control) = (fluorescence maximum after peptide or buffer application − fluorescence (baseline))/(fluorescence before application − fluorescence (baseline)) × 100%. The results are presented as the mean ± S.D.; $n = 15$ (buffer), $n = 30$ (Ms 9a-1); ***, $p < 0.001$. Statistical significance was evaluated by two-tailed *t* test.

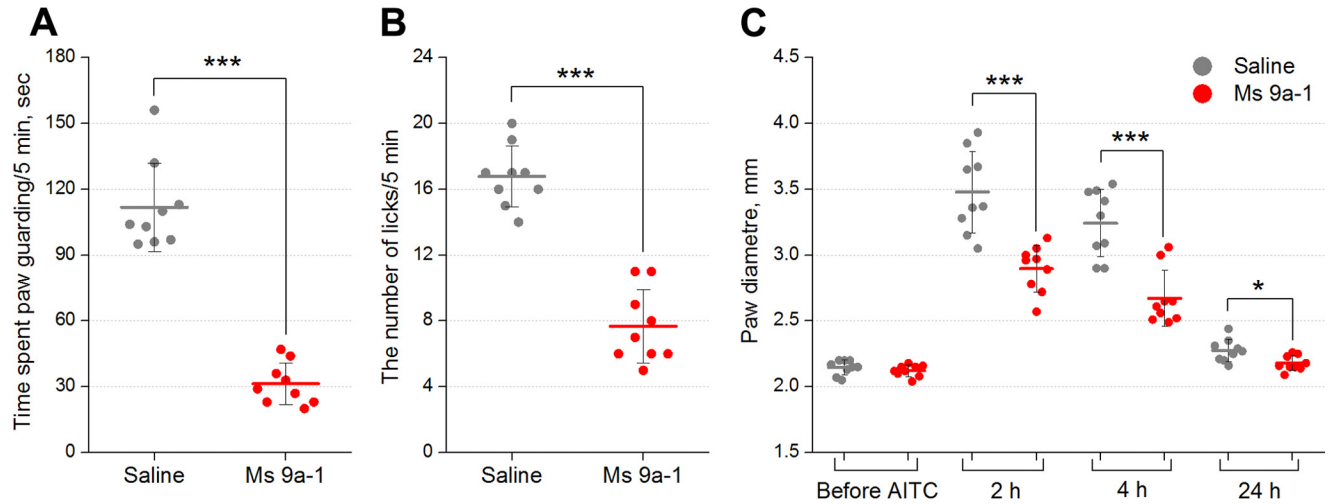

FIGURE 7. ***In vivo* efficacy of Ms 9a-1 in AITC-induced pain model.** Pretreatment of mice with peptide Ms 9a-1 (0.3 mg/kg i.v.) attenuated the response to AITC. Ms 9a-1 significantly reduced time spent paw guarding (*A*) and the number of paw licks (*B*) within a 5-min interval after AITC injection. *C*, Ms 9a-1 (0.3 mg/kg i.v.) significantly decreased development of paw edema after AITC injection. The results are presented as the mean ± S.D., $n = 9$ for each group; ***, $p < 0.001$; *, $p < 0.05$, *versus* saline group (ANOVA followed by a Tukey's test).

probably Ms 9a-1 produces the significant analgesic effect *in vivo* via a reduced response of TRPA1-expressing neurons to stimuli. Endogenously produced agonists, such as reactive oxygen species (15), prostaglandins (17, 47), the small endogenous gasotransmitters NO (48) and H_2S (49), and nitroxyl anion (HNO) (50), are not able to induce significant activation of

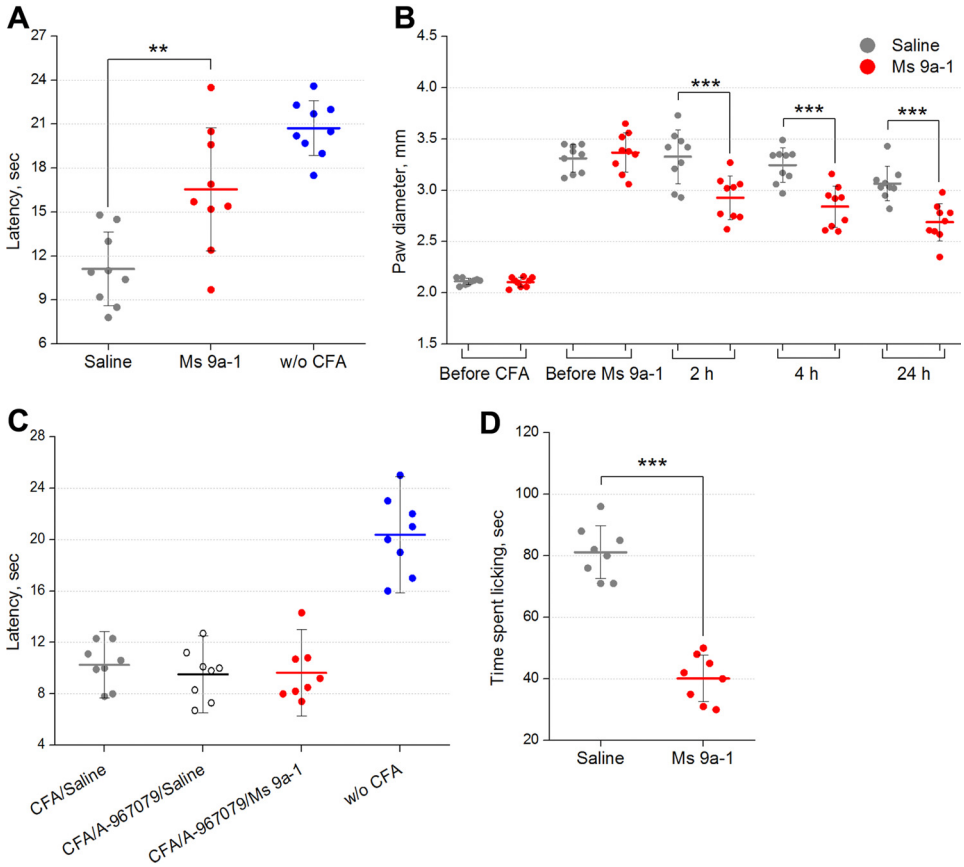

FIGURE 8. **Efficacy of Ms 9a-1 in CFA and capsaicin tests.** *A*, the effect of peptide Ms 9a-1 (0.3 mg/kg i.v.) on mice withdrawal latency from a hot plate in the thermal hyperalgesia test after CFA injection ($n = 9$ for each group). *B*, effect of Ms 9a-1 (0.3 mg/kg i.v.) on CFA-induced paw edema ($n = 9$ for each group). *C*, selective TRPA1 antagonist A-967079 (20 mg/kg, p.o.) reversed the effect of peptide Ms 9a-1 (0.3 mg/kg, i.v.) on thermal hyperalgesia ($n = 8$ for each group). *D*, 0.3 mg/kg dose of Ms 9a-1 significantly reduced the behavioral response to capsaicin ($n = 8$ for each group). The results are presented as the mean ± S.D.; ***, $p < 0.001$; **, $p < 0.01$, *versus* saline group (ANOVA followed by a Tukey's test).

TRPA1 at physiological concentrations, but Ms 9a-1 could potentiate this activation (Fig. 6) and desensitize neurons expressing TRPA1 in the same way as reported for p-BQ, NAPQI, or parthenolide. Desensitized neurons are unable to respond to AITC, a selective agonist of TRPA1, which corresponds with the significant inhibition of mice reaction to AITC. The same effect was achieved after administration of the selective antagonist of TRPA1 at high doses (35).

Interestingly, Ms 9a-1 produced dissimilar effects with a low molecular weight TRPA1 antagonist in CFA testing. In contrast to Ms 9a-1, TRPA1 antagonists HC-030031 and A-967079 were unable to reverse CFA-induced thermal hyperalgesia (40, 51). Therefore, the *in vivo* effects of Ms 9a-1 are distinct from the inhibition of TRPA1 receptors. It is established that the vanilloid receptor TRPV1 is expressed in the most TRPA1-expressing DRG neurons (5, 34), and it is considered to play a leading role in the development of CFA-induced thermal hyperalgesia (52). As was shown before, mustard oil (agonist of TRPA1) in peripheral nociceptors cause desensitization of response to capsaicin as was shown using an *in vitro* neuropeptide release assay from acutely isolated rat hind paw skin preparation and *in vivo* behavioral assays (53). And the data on MS 9a-1 inhibition of capsaicin-induced pain behavior (Fig. 8*D*) correspond well with that reported in this study desensitization of response to capsaicin after pretreatment with TRPA1 agonist (mustard oil) (53).

Moreover, parthenolide, a partial agonist of TRPA1, was shown to block the response to a selective agonist of TRPV1, capsaicin, via desensitization of TRPA1-expressing neurons (46). Intrathecal injection of the TRPA1 agonists cinnamaldehyde, NAPQI, and p-BQ produced a dose-dependent and reversible increase in paw withdrawal latency in a hot-plate test (3). Therefore, desensitization of TRPA1-expressing neurons could lead to inhibition of response to capsaicin and the reversal of inflammation and thermal hyperalgesia induced by CFA.

Administration of selective TRPA1 antagonist A-967079 completely blocked the effect of Ms 9a-1 on CFA-induced thermal hyperalgesia (Fig. 8*C*). Therefore, activation of TRPA1 is essential for the analgesic effect of the peptide.

To date the list of polypeptide molecules affecting TRPA1 has been limited to the peptide toxin t-ProTx-I (W5A), which was constructed on the base of a 35-residue peptide from the venom of the Peruvian green-velvet tarantula *Thrixopelma pruriens*, which also significantly inhibits $Na_v1.2$ (54). Ms 9a-1 does not have any homology to this peptide but instead has the boundless β-hairpin peptide fold characteristic of group 9a sea anemone toxins (23). All peptides of this group are encoded as part of complex polypeptide precursors. In the case of Ms 9a-1, we found two precursors, each consisting of the signal peptide, the spacer region, the active peptide Ms 9a-1, and one additional peptide, Ms 9a-2 or Ms 9a-3. The production of complex precursors is an effective way for intensive expression of short

peptides in animals and plants (23, 55). For animals, the most pronounced example is the expression of the peptide toxin Am-1, which possesses weak lethal activity toward crabs (LD_{50} 830 g/kg) and contains 6 copies of this peptide in the precursor protein (56).

Peptide Ms 9a-1 evidently differs from homologous sea anemone peptides (Fig. 2*C*) by extended C termini that probably appeared due to a mutation of a dipeptidyl peptidase processing site (DP or EP). Such a mutation could be responsible for the appearance of TRPA1-potentiating activity, but further experiments are needed to confirm this suggestion. Ms 9a-1 could be a starting point for docking experiments, mutagenesis, and peptide mimetic design as the structure of TRPA1 was recently determined by electron cryo-microscopy (57).

We should conclude that τ-AnmTX Ms 9a-1 possesses unique properties; it acts as a positive modulator, significantly potentiating TRPA1 response to different agonists *in vitro*, and produces significant antinociceptive and anti-inflammatory effects *in vivo*. Therefore, τ-AnmTX Ms 9a-1 could represent a new therapeutic strategy; that is, potentiating TRPA1 and leading to inhibition of the neurogenic inflammatory response, most probably due to desensitization of TRPA1-positive neurons. Potentiating the receptor with such a beneficial outcome is attractive as currently existing inhibitors of TRPA1 have too-high effective doses (Ed_{50} >20 mg/kg) (40, 51), whereas known partial agonists cause pain. Moreover, τ-AnmTX Ms 9a-1 could serve as a research tool to determine the involvement of these neurons in physiological and pathological states.

Materials and Methods

Venom Collection—M. senile specimens were collected off the coast, near Tromsø, Norway in September 2012 and kept in fresh-flowing seawater at 12 °C for some days. The venom of *M. senile* was collected from living specimens by using electrical impulses impact (160 mA, 10 Hz). The mucus released by the anemone specimens was washed out with 10 mM EDTA, 1 mM PMSF solution.

Purification Procedure—Salt was removed from the samples of the venom by solid phase extraction. The sample was loaded onto Sep-Pak C_{18} Vac cartridge/5000 mg (Waters) equilibrated in buffer A (0.1% trifluoroacetic acid (TFA)). After washing with buffer A, elution was performed with 70% acetonitrile (ACN) solution containing 0.1% TFA. The non-bound material was discarded. The collected eluate was lyophilized and kept frozen at −20 °C until further separation by HPLC. The first stage of HPLC separation was done on a reverse-phase column Jupiter C_5 (250 × 10 mm, Phenomenex) using a linear gradient (0–60% in 60 min) of ACN in the presence of 0.1% TFA and a constant flow rate 5 ml/min (Fig. 1*A*). On the second stage the Ms 9a-1 peptide was purified on Synergi Fusion-RP column (250 × 3 mm, Phenomenex) using a linear gradient (0–30% in 1 min, 30–50% in 30 min) of ACN concentration in the presence of 0.1% TFA and a constant flow rate 0.5 ml/min (Fig. 1*B*).

Mass Spectrometry—MALDI time-of-flight spectrometry on an Ultraflex TOF-TOF instrument (Burker Daltonik, Bremen, Germany) was used to measure molecular weight. Calibration was performed with either a ProteoMass peptide and protein MALDI-MS calibration kit or a ProteoMass peptide MALDI-MS calibration kit, with mass ranges 700–66,000 Da and 700–3,500 Da, respectively (Sigma). The molecular mass determination was carried out in a linear or reflector positive ion mode. Samples were prepared by using the dried-droplet method with 2.5-dihydroxybenzoic acid (10 mg/ml in 70% ACN solution with 0.1% TFA) or α-cyano-4-hydroxycinnamic acid (10 mg/ml in 50% ACN solution with 0.1% TFA) as a matrix.

Reduction of Disulfide Bonds and Modification of Thiol Groups—Lyophilized peptide was dissolved in 40 μl of denaturation buffer containing 100 mM Tris-HCl, pH 8.0, 6 M guanidine-HCl, and 3 mM EDTA. Disulfide bonds were reduced by incubation for 4 h at 40 °C with 2 μl of 1.2 M 1,4-dithiothreitol. Free thiol groups were alkylated by the addition of 2 μl of 50% 4-vinylpyridine in methanol and incubation at room temperature in the dark for 15 min. The modified peptide was immediately isolated from reducing and alkylating agents by HPLC on reverse-phase column Luna C_{18} (150 mm × 3 mm, Phenomenex) using a linear gradient (10–50% in 40 min) of ACN solution containing 0.1% TFA and a constant flow rate 0.3 ml/min.

Amino acid Sequence Analysis—Alkylated peptide was partially analyzed by automated stepwise Edman degradation method on a Procise model 492 protein sequencer (Applied Biosystems) according to the manufacturers' protocol.

Precursor Determination—Total RNA was isolated from the tentacles of *M. senile* using TRIsol® reagent (Ambion) and the manufacturer's protocol. Reverse transcription of RNA into cDNA was performed using the MINT kit (Evrogen, Moscow, Russia) according to the manufacturer's recommendations. 3′-Terminus determination was carried out by 3′-RACE using the universal primer T7cap (GTA ATA CGA CTC ACT ATA GGG CAA GCA GTG GTA ACA ACG CAG AGT) and degenerated primers MS-d1 (GTA GGA GGN TGY ATH AAR TGY CA) and MS-d2 (GGT CGA TGT GTG AGN ATH GTN GG). 5′-RACE was performed with universal primer T7cap and reverse primers MS-r1 (ACA GCC GGC GAT ACG AAC ACA) and MS-r2 (CCA TTG GAA TCT TGT GTA TGA C). Full precursor sequences were synthesized by PCR using primers MS-5′-end (GTC AAC TGA GAC CTA CAA CAC) and MS-3′-end (CAA TTA TGA ATG GTT ATA GAT CCC). DNA sequencing was performed on Applied Biosystems 3730 DNA Analyzer.

Gene Synthesis—The DNA sequence encoding peptide Ms 9a-1 was constructed by PCR technique using four synthetic oligonucleotides: MS-dir1 (TAG AAT TCA TGA ATA TTA TTG TGG GCG GCT GCA TTA AAT G) containing the Met codon for BrCN cleavage, MS-dir2 (GGG CGG CTG CAT TAA ATG CCA TGT GAA AAA TGC GTC CGG CCG TTG), MS-rev1 (GAC TCG AGC TAG GAA AAC AGA TCC GGC ACT TTA TCC ACG CCG CA), and MS-rev2 (CAC TTT ATC CAC GCC GCA GCC CAC AAT ACG CAC GCA ACG GCC GGA CGC AT). The amplified PCR fragment was gel-purified and cloned into the expression vector pET32b+ (Novagen) digested with restriction enzyme EcoRV (Fermentas, Vilnius, Lithuania).

Recombinant Peptide Production—Recombinant peptide Ms 9a-1 was produced as a thioredoxin fusion protein in *E. coli* BL21(DE3). Cells were transformed with the expression vector

and cultivated in LB medium with ampicillin (100 μg/ml) at 37 °C. When the culture density reached $A_{600} \sim 0.6-0.8$, isopropyl-1-thio-β-D-galactopyranoside was added up to 0.2 mM to induce expression. After cultivation for 18 h at 25 °C, cells were centrifuged (5 min at 6000 × *g*), resuspended in a buffer for metal affinity chromatography (400 mM NaCl, 20 mM Tris-HCl, pH 7.5), and ultrasonicated. To remove all insoluble particles, the extract was centrifuged for 15 min at 9000 × *g*. The supernatant was purified using TALON Superflow metal affinity resin (Clontech) using manufacturer protocols. Thioredoxin fusion protein was cleaved in the dark at room temperature by BrCN with the addition of HCl up to 0.2 M, as described previously (32). The BrCN molar ratio to protein was 600:1. The target peptide was isolated from the reaction mixture using a reverse-phase column Jupiter C_5 (250 × 10 mm). The purity of recombinant peptide was confirmed by N-terminal sequencing and MALDI-TOF mass spectrometry.

Fluorescent Assay of Calcium Influx—Initially the CHO cell line stably expressing rat TRPA1 (rTRPA1, AY496961.1) was produced using the T-Rex System (Invitrogen) according to the manufacturer's protocol. cDNA-encoding rTRPA1 was cloned into vector pcDNA4/TO, which provides inducible expression in mammalian cell lines. The CHO cells that carried the regulatory vector pcDNA6/TR encoding the tetracycline repressor were transfected with the pcDNA4/TO-rTRPA1 plasmid, and after 2 weeks of selection by blasticidin (5 μg/ml) and zeocin (250 μg/ml) single colonies were screened using the agonist-induced Ca^{2+} uptake assay. TRPA1 expression was induced by tetracycline, adding up to 1 μg/ml 24 h before testing. Positive clones were expanded and used. Fluorescent assays were performed using a tablet spectrophotometer with the integrated automatic liquid dosing system NOVOstar (BMG LABTECH, Ortenberg, Germany). rTRPA1-CHO cells were seeded into black-walled, clear-bottomed 96-well plates at a density of 75,000 cells per well and cultured overnight at 37 °C (complete media without antibiotics containing 1 μg/ml tetracycline). TRPA1-expressing cells were stained with the cytoplasmic calcium indicator Fluo-4AM using Fluo-4 Direct™ calcium assay kits (Invitrogen) and incubated in the dark at 37 °C and 25 °C for 60 min each. The control (buffer alone) and serial dilutions of the peptide were added to the cells, and immediately the measurement was carried out. Fluorescent signals (λex = 485 nM, λem = 520 nM) were monitored before and after the addition of the TRPA1 agonist (100 μM AITC). The measurements were performed at room temperature and pH 7.4.

Calcium Imaging of DRG Neurons—Animal care and animal experiments were performed following the protocol approved by the Animal Care and Use Committee of the Shemyakin-Ovchinnikov Institute of Bioorganic Chemistry, RAS (protocol 191/2015). Male adult (3 months old) Wistar rats were used. They were kept under a 12-h light-dark cycle with free access to chow and water. Rats were deeply anesthetized by inhalation of isoflurane (Baxter Healthcare Corp.), and DRGs from segmental levels T1-L5 were excised.

The culturing procedure was performed as described earlier (58) with some modifications. Isolated DRGs were incubated in an enzyme mixture (2 mg/ml collagenase type 1 and 2 mg/ml dispase II (Sigma)) in calcium-, magnesium-free Hanks' balanced salt solution (Paneco, Moscow, Russia) for 15 min at 37 °C, and neurons were dissociated by trituration with a glass Pasteur pipette. This step was repeated 3 times, and then cells were washed by centrifugation (3 times at 1000 × *g* for 2 min) in L15 medium (Sigma) containing 10% fetal bovine serum. After the final washing step cells were suspended in basal TNB-100 medium supplemented with lipid-protein complex (Biochrom AG, Berlin, Germany) and 25 μM cytosine β-D-arabinofuranoside (Sigma). The cell suspension was transferred onto poly-D-lysine/laminin (Sigma)-coated 96-well cell culture plates (cells obtained from 0.5–1 ganglia/well) and cultured for 20–24 h in CO_2 incubator.

The intracellular calcium concentration ($[Ca^{2+}]_i$) measurements were performed using primary cultures of DRG neurons. Measurements were done in a buffer ECS, pH 7.4, containing 140 mM NaCl, 2.8 mM KCl, 4 mM $MgCl_2$, 2 mM $CaCl_2$, 20 mM HEPES, 10 mM D-glucose at room temperature. The cells were loaded with 2 μM Fluo-4AM and 1.25 mM probenecid (Invitrogen) in the buffer for 30 min at 37 °C and then for 30 min at room temperature. Fluo-4 was excited at 460–495-nm wavelengths, and fluorescence was collected at 510–550 nm with a fluorescent microscope Olympus IX71 (Olympus, Tokyo, Japan). Individual cell responses were recorded using XM10 monochrome camera and Cell A imaging software (Olympus), and changes in fluorescence levels were analyzed with ImageJ software. Each cell was tracked independently, and the fluorescence intensity at the beginning of the experiment was set to 100%. In each experiment the cells were exposed to the ECS buffer and TRPA1 agonist AITC (75 μM) followed by peptide Ms 9a-1 (300 nM) and capsaicin (0.5 μM) applications. To exclude the effect of mechanical impact on DRG cells, buffer instead of the peptide was used or buffer was followed by AITC and capsaicin applications. To show that the peptide alone had no effect on the cells, it was applied before agonist and capsaicin applications. All ligands except Ms 9a-1 were purchased from Sigma.

Electrophysiology—rTRPA1 (AY496961.1) cRNA was synthesized from the NarI-linearized pVAX1/TRPA1 plasmid using TranscriptAid™ T7 High Yield Transcription kit (Fermentas) according to the manufacturer's protocol for capped transcripts. *X. laevis* oocytes were dissected from frog and defolliculated by shaking at room temperature for 120 min in the sterile solution containing 100 mM NaCl, 2.5 mM KCl, 1 mM $MgCl_2$, 5 mM HEPES, pH 7.4, laced with 1 mg/ml collagenase. Intact oocytes were injected with 2–5 ng of cRNA transcript. Injected oocytes were incubated for 2–7 days at 15–19 °C in sterile ND-96 medium containing 100 mM NaCl, 2.5 mM KCl, 1.8 mM $CaCl_2$, 1 mM $MgCl_2$, 5 mM HEPES, pH 7.4, supplemented with 50 μg/ml gentamycin. cRNA-injected oocytes were placed in a special bath perfused with a Ca^{2+}-free solution that contained 100 mM NaCl, 2.5 mM KCl, 1 mM $MgCl_2$, 5 mM HEPES, pH 7.4. Then oocytes were impaled with two glass microelectrodes filled with 3 M KCl connected to a GeneClamp 500 amplifier (Axon Instruments). Oocytes were clamped at −20 mV, recording both inward/outward currents made at repeated steps to −80 mV for 80 ms following voltage ramp from −80 mV to +80 mV for 200 ms every 4 s. For outward currents recording oocytes were clamped at −20 mV, and

recordings of activation were made at repeated voltage step to +80 mV for 200 ms every 4 s. Diclofenac (300 μM in Ca^{2+}-free solution) (2) or AITC (100 μM in Ca^{2+}-free solution) (59) was added to the bath with oocytes to activate the channel. Experiments were performed at room temperature (22–24 °C). The data were filtered at 20 Hz and digitized at 100 Hz by an AD converter L780 (LCard, Moscow, Russia) using in-house software. For curve-fitting analysis we used a four-parameter logistic equation, $F(x) = A2 + (A1 - A2)/(1 + (x/x_0)$ p), where x is the concentration of peptide, $F(x)$ is the response value at a given peptide concentration, $A2$ is the maximal response value (% of control), $A1$ is the control response value (fixed at 100%), x_0 is the EC_{50} value, and p is the Hill coefficient (slope factor).

Animal Models—Adult male CD-1 mice (20–25 g; Animal Breeding Facility Branch of Shemyakin-Ovchinnikov Institute of Bioorganic Chemistry, Russian Academy of Sciences, Pushchino, Russia) were housed at room temperature (23 ± 2 °C) and subjected to a 12-h light-dark cycle with food and water available *ad libitum*. Experiments were approved by the Animal Care and Use Committee of the Branch of the IBCh RAS (Pushchino, Russia). Each animal was used only once and was euthanized in the CO_2 chamber immediately after the completion of the experiment. In all nociceptive and behavioral tests, the responses were recorded by a person blind to the treatment. Ms 9a-1 was dissolved in saline. The significance of the data was determined by one-way analysis of variance followed by a Tukey's post hoc test. Data are presented as the mean ± S.D.

Test on Pain/Thermal Hyperalgesia-evoking Activity—Ms 9a-1 (2.5 μg/10 μl) or saline (10 μl) was injected in a left hind paw. Licking or guarding of injected paw was monitored. The latency of left hind paw withdraw from the hot plate (53 °C) was measured 2 h after injection.

Open Field Test—Open-field activity was measured using TSE Multi Conditioning System Extended Advanced with TSE ActiMot (Activity and Hole Board Measuring System) module and test arena "Open field" (TSE Systems, Inc., Chesterfield, MO). Spontaneous locomotor activity was recorded for 15 min. Peptide and saline were administered i.v. 30 min before testing.

AITC-induced Pain and Inflammation—The AITC-induced nocifensive behavioral response was evoked by the injection of AITC (20 μl, 0.5% in saline) into the plantar surface of the left hind paw. Ms 9a-1 or saline were administrated i.v. 30 min before AITC administration. The control mice were treated by 20 μl of saline. The number of licks and duration of paw guarding for 5 min after injection of AITC were recorded. The extent of paw edema was evaluated before the test and 2, 4, and 24 h after AITC injection using an electronic digital caliper.

Complete Freund's Adjuvant-induced Thermal Hyperalgesia and Inflammation—The thermal hyperalgesia was induced using CFA. CFA was suspended in oil/saline (1:1) emulsion. Mice were injected with 20 μl of CFA emulsion into the plantar surface of the left hind paw 24 h before i.v. sample administration. Control mice were injected with 20 μl of saline. Testing was performed 30 min after peptide or saline administration. The latency of paw withdrawal was determined upon thermal stimulation on a hot plate (53 °C) 24 h after CFA injection. The paw edema was evaluated before CFA injection before and 2, 4, and 24 h after Ms 9a-1 or saline administration using the electronic digital caliper. TRPA1 antagonist A-967079 (Sigma) was dissolved in 85% PEG400 and administrated orally (20 mg/kg, p.o.).

Capsaicin Test—Intraplantar injection of capsaicin (3 μg/10 μl in 10% ethanol/90% saline) was used to elicit capsaicin-induced acute pain. Immediately after the capsaicin injection, mice were placed inside glass cylinders for observation for 15 min. The duration of episodes of paw licking was recorded.

Computation—The similarity of the mature chain sequences was determined by both a BLAST search (blast.ncbi.nlm.nih.gov) and by SRDA (60–62). The sequence and spatial structure data for analyses were retrieved from the UniProt Data Bank. The Sequence alignment was built by the Megalign module from Dnastar Inc.

Author Contributions—Y. A. L. and Y. A. A. designed the study and wrote the paper. Y. A. L., S. A. K., K. S., and Y. A. A. analyzed and critically evaluated the results. I. V. M. and Y. V. K. performed Ca^{2+} imaging experiments with TRPA1-expressing cells. Y. A. L. and I. V. S. performed Ca^{2+} imaging experiments on DRG neurons. I. A. D., V. A. P., Y. A. P., and A. N. M. designed and performed the experiments on mice. K. S. and Y. A. A. collected venom from sea anemones. Y. A. L. performed all the experiments on peptide isolation, recombinant peptide production, and oocyte electrophysiology. Y. A. A. performed all DNA and RNA manipulations. All authors read and approved the final version of the manuscript.

Acknowledgments—We thank Runar Gjerp Sostad and Prof. Tor Haug (Norwegian College of Fishery Science, University of Tromsø, Tromsø, Norway) for assistance in the collection of M. senile venom. We also acknowledge Dr. Sergey G. Koshelev (Shemyakin-Ovchinnikov Institute of Bioorganic Chemistry, Russian Academy of Sciences, Moscow, Russia) for assistance in electrophysiological experiments.

References

1. Caterina, M. J. (2007) Chemical biology: sticky spices. *Nature* **445,** 491–492
2. Hu, H., Tian, J., Zhu, Y., Wang, C., Xiao, R., Herz, J. M., Wood, J. D., and Zhu, M. X. (2010) Activation of TRPA1 channels by fenamate nonsteroidal anti-inflammatory drugs. *Pflugers Arch.* **459,** 579–592
3. Andersson, D. A., Gentry, C., Alenmyr, L., Killander, D., Lewis, S. E., Andersson, A., Bucher, B., Galzi, J. L., Sterner, O., Bevan, S., Högestätt, E. D., and Zygmunt, P. M. (2011) TRPA1 mediates spinal antinociception induced by acetaminophen and the cannabinoid Δ(9)-tetrahydrocannabiorcol. *Nat. Commun.* **2,** 551
4. Zhou, Y., Suzuki, Y., Uchida, K., and Tominaga, M. (2013) Identification of a splice variant of mouse TRPA1 that regulates TRPA1 activity. *Nat. Commun.* **4,** 2399
5. Andrè, E., Campi, B., Materazzi, S., Trevisani, M., Amadesi, S., Massi, D., Creminon, C., Vaksman, N., Nassini, R., Civelli, M., Baraldi, P. G., Poole, D. P., Bunnett, N. W., Geppetti, P., and Patacchini, R. (2008) Cigarette smoke-induced neurogenic inflammation is mediated by α,β-unsaturated aldehydes and the TRPA1 receptor in rodents. *J. Clin. Invest.* **118,** 2574–2582
6. Andrè, E., Gatti, R., Trevisani, M., Preti, D., Baraldi, P. G., Patacchini, R., and Geppetti, P. (2009) Transient receptor potential ankyrin receptor 1 is a novel target for pro-tussive agents. *Br. J. Pharmacol.* **158,** 1621–1628
7. Birrell, M. A., Belvisi, M. G., Grace, M., Sadofsky, L., Faruqi, S., Hele, D. J., Maher, S. A., Freund-Michel, V., and Morice, A. H. (2009) TRPA1 agonists evoke coughing in guinea pig and human volunteers. *Am. J. Respir. Crit. Care Med.* **180,** 1042–1047

8. Namer, B., Seifert, F., Handwerker, H. O., and Maihöfner, C. (2005) TRPA1 and TRPM8 activation in humans: effects of cinnamaldehyde and menthol. *Neuroreport* **16,** 955–959
9. Macpherson, L. J., Geierstanger, B. H., Viswanath, V., Bandell, M., Eid, S. R., Hwang, S., and Patapoutian, A. (2005) The pungency of garlic: activation of TRPA1 and TRPV1 in response to allicin. *Curr. Biol.* **15,** 929–934
10. Taylor-Clark, T. E., Ghatta, S., Bettner, W., and Undem, B. J. (2009) Nitrooleic acid, an endogenous product of nitrative stress, activates nociceptive sensory nerves via the direct activation of TRPA1. *Mol. Pharmacol.* **75,** 820–829
11. Hu, H., Bandell, M., Petrus, M. J., Zhu, M. X., and Patapoutian, A. (2009) Zinc activates damage-sensing TRPA1 ion channels. *Nat. Chem. Biol.* **5,** 183–190
12. Bessac, B. F., Sivula, M., von Hehn, C. A., Escalera, J., Cohn, L., and Jordt, S. E. (2008) TRPA1 is a major oxidant sensor in murine airway sensory neurons. *J. Clin. Invest.* **118,** 1899–1910
13. Satoh, J., and Yamakage, M. (2009) Desflurane induces airway contraction mainly by activating transient receptor potential A1 of sensory C-fibers. *J. Anesth.* **23,** 620–623
14. Eilers, H., Cattaruzza, F., Nassini, R., Materazzi, S., Andre, E., Chu, C., Cottrell, G. S., Schumacher, M., Geppetti, P., and Bunnett, N. W. (2010) Pungent general anesthetics activate transient receptor potential-A1 to produce hyperalgesia and neurogenic bronchoconstriction. *Anesthesiology* **112,** 1452–1463
15. Trevisani, M., Siemens, J., Materazzi, S., Bautista, D. M., Nassini, R., Campi, B., Imamachi, N., Andrè, E., Patacchini, R., Cottrell, G. S., Gatti, R., Basbaum, A. I., Bunnett, N. W., Julius, D., and Geppetti, P. (2007) 4-Hydroxynonenal, an endogenous aldehyde, causes pain and neurogenic inflammation through activation of the irritant receptor TRPA1. *Proc. Natl. Acad. Sci. U.S.A.* **104,** 13519–13524
16. Taylor-Clark, T. E., McAlexander, M. A., Nassenstein, C., Sheardown, S. A., Wilson, S., Thornton, J., Carr, M. J., and Undem, B. J. (2008) Relative contributions of TRPA1 and TRPV1 channels in the activation of vagal bronchopulmonary C-fibres by the endogenous autacoid 4-oxononenal. *J. Physiol.* **586,** 3447–3459
17. Taylor-Clark, T. E., Undem, B. J., Macglashan, D. W., Jr., Ghatta, S., Carr, M. J., and McAlexander, M. A. (2008) Prostaglandin-induced activation of nociceptive neurons via direct interaction with transient receptor potential A1 (TRPA1). *Mol. Pharmacol.* **73,** 274–281
18. Cruz-Orengo, L., Dhaka, A., Heuermann, R. J., Young, T. J., Montana, M. C., Cavanaugh, E. J., Kim, D., and Story, G. M. (2008) Cutaneous nociception evoked by 15-ΔPGJ2 via activation of ion channel TRPA1. *Mol. Pain* **4,** 30
19. Andreev, Y. A., Vassilevski, A. A., and Kozlov, S. A. (2012) Molecules to selectively target receptors for treatment of pain and neurogenic inflammation. *Recent Pat. Inflamm. Allergy Drug Discov.* **6,** 35–45
20. Jouiaei, M., Yanagihara, A. A., Madio, B., Nevalainen, T. J., Alewood, P. F., and Fry, B. G. (2015) Ancient venom systems: a review on Cnidaria toxins. *Toxins* **7,** 2251–2271
21. Chi, V., Pennington, M. W., Norton, R. S., Tarcha, E. J., Londono, L. M., Sims-Fahey, B., Upadhyay, S. K., Lakey, J. T., Iadonato, S., Wulff, H., Beeton, C., and Chandy, K. G. (2012) Development of a sea anemone toxin as an immunomodulator for therapy of autoimmune diseases. *Toxicon* **59,** 529–546
22. Kozlov, S. A., Osmakov, D. I., Andreev, I. a. A., Koshelev, S. G., Gladkikh, I. N., Monastyrnaia, M. M., Kozlovskaia, E. P., and Grishin, E. (2012) Polypeptide toxin from sea anemone inhibiting proton-sensitive channel ASIC3. *Bioorg. Khim.* **38,** 653–659
23. Osmakov, D. I., Kozlov, S. A., Andreev, Y. A., Koshelev, S. G., Sanamyan, N. P., Sanamyan, K. E., Dyachenko, I. A., Bondarenko, D. A., Murashev, A. N., Mineev, K. S., Arseniev, A. S., and Grishin, E. (2013) Sea anemone peptide with uncommon β-hairpin structure inhibits acid-sensing ion channel 3 (ASIC3) and reveals analgesic activity. *J. Biol. Chem.* **288,** 23116–23127
24. Diochot, S., Baron, A., Rash, L. D., Deval, E., Escoubas, P., Scarzello, S., Salinas, M., and Lazdunski, M. (2004) A new sea anemone peptide, APETx2, inhibits ASIC3, a major acid-sensitive channel in sensory neurons. *EMBO J.* **23,** 1516–1525
25. Andreev, Y. A., Kozlov, S. A., Korolkova, Y. V., Dyachenko, I. A., Bondarenko, D. A., Skobtsov, D. I., Murashev, A. N., Kotova, P. D., Rogachevskaja, O. A., Kabanova, N. V., Kolesnikov, S. S., and Grishin, E. (2013) Polypeptide modulators of TRPV1 produce analgesia without hyperthermia. *Mar. Drugs* **11,** 5100–5115
26. Andreev, Y. A., Kozlov, S. A., Kozlovskaya, E. P., and Grishin, E. (2009) Analgesic effect of a polypeptide inhibitor of the TRPV1 receptor in noxious heat pain models. *Dokl. Biochem. Biophys.* **424,** 46–48
27. Kozlov, S., and Grishin, E. (2012) Convenient nomenclature of cysteine-rich polypeptide toxins from sea anemones. *Peptides* **33,** 240–244
28. Kozlov, S. A., and Grishin, E. (2007) The universal algorithm of maturation for secretory and excretory protein precursors. *Toxicon* **49,** 721–726
29. Cassoli, J. S., Verano-Braga, T., Oliveira, J. S., Montandon, G. G., Cologna, C. T., Peigneur, S., Pimenta, A. M., Kjeldsen, F., Roepstorff, P., Tytgat, J., and de Lima, M. E. (2013) The proteomic profile of *Stichodactyla duerdeni* secretion reveals the presence of a novel *O*-linked glycopeptide. *J. Proteomics* **87,** 89–102
30. Zaharenko, A. J., Ferreira, W. A., Jr., Oliveira, J. S., Richardson, M., Pimenta, D. C., Konno, K., Portaro, F. C., and de Freitas, J. C. (2008) Proteomics of the neurotoxic fraction from the sea anemone *Bunodosoma cangicum* venom: novel peptides belonging to new classes of toxins. *Comp. Biochem. Physiol. Part D Genomics Proteomics* **3,** 219–225
31. Honma, T., Kawahata, S., Ishida, M., Nagai, H., Nagashima, Y., and Shiomi, K. (2008) Novel peptide toxins from the sea anemone *Stichodactyla haddoni*. *Peptides* **29,** 536–544
32. Andreev, Y. A., Kozlov, S. A., Vassilevski, A. A., and Grishin, E. (2010) Cyanogen bromide cleavage of proteins in salt and buffer solutions. *Anal. Biochem.* **407,** 144–146
33. Andreev, Y. A., Kozlov, S. A., Koshelev, S. G., Ivanova, E. A., Monastyrnaya, M. M., Kozlovskaya, E. P., and Grishin, E. (2008) Analgesic compound from sea anemone *Heteractis crispa* is the first polypeptide inhibitor of vanilloid receptor 1 (TRPV1). *J. Biol. Chem.* **283,** 23914–23921
34. Bautista, D. M., Jordt, S. E., Nikai, T., Tsuruda, P. R., Read, A. J., Poblete, J., Yamoah, E. N., Basbaum, A. I., and Julius, D. (2006) TRPA1 mediates the inflammatory actions of environmental irritants and proalgesic agents. *Cell* **124,** 1269–1282
35. McNamara, C. R., Mandel-Brehm, J., Bautista, D. M., Siemens, J., Deranian, K. L., Zhao, M., Hayward, N. J., Chong, J. A., Julius, D., Moran, M. M., and Fanger, C. M. (2007) TRPA1 mediates formalin-induced pain. *Proc. Natl. Acad. Sci. U.S.A.* **104,** 13525–13530
36. Chen, Y., Yang, C., and Wang, Z. J. (2011) Proteinase-activated receptor 2 sensitizes transient receptor potential vanilloid 1, transient receptor potential vanilloid 4, and transient receptor potential ankyrin 1 in paclitaxel-induced neuropathic pain. *Neuroscience* **193,** 440–451
37. Kremeyer, B., Lopera, F., Cox, J. J., Momin, A., Rugiero, F., Marsh, S., Woods, C. G., Jones, N. G., Paterson, K. J., Fricker, F. R., Villegas, A., Acosta, N., Pineda-Trujillo, N. G., Ramírez, J. D., Zea, J., *et al.* (2010) A gain-of-function mutation in TRPA1 causes familial episodic pain syndrome. *Neuron* **66,** 671–680
38. Brierley, S. M., Castro, J., Harrington, A. M., Hughes, P. A., Page, A. J., Rychkov, G. Y., and Blackshaw, L. A. (2011) TRPA1 contributes to specific mechanically activated currents and sensory neuron mechanical hypersensitivity. *J. Physiol.* **589,** 3575–3593
39. Schwartz, E. S., La, J. H., Scheff, N. N., Davis, B. M., Albers, K. M., and Gebhart, G. F. (2013) TRPV1 and TRPA1 antagonists prevent the transition of acute to chronic inflammation and pain in chronic pancreatitis. *J. Neurosci.* **33,** 5603–5611
40. Chen, J., Joshi, S. K., DiDomenico, S., Perner, R. J., Mikusa, J. P., Gauvin, D. M., Segreti, J. A., Han, P., Zhang, X. F., Niforatos, W., Bianchi, B. R., Baker, S. J., Zhong, C., Simler, G. H., McDonald, H. A., *et al.* (2011) Selective blockade of TRPA1 channel attenuates pathological pain without altering noxious cold sensation or body temperature regulation. *Pain* **152,** 1165–1172
41. Eid, S. R., Crown, E. D., Moore, E. L., Liang, H. A., Choong, K. C., Dima, S., Henze, D. A., Kane, S. A., and Urban, M. O. (2008) HC-030031, a TRPA1

selective antagonist, attenuates inflammatory- and neuropathy-induced mechanical hypersensitivity. *Mol. Pain* **4,** 48
42. Preti, D., Saponaro, G., and Szallasi, A. (2015) Transient receptor potential ankyrin 1 (TRPA1) antagonists. *Pharm. Pat. Anal.* **4,** 75–94
43. Brederson, J. D., Kym, P. R., and Szallasi, A. (2013) Targeting TRP channels for pain relief. *Eur. J. Pharmacol.* **716,** 61–76
44. Kojima, R., Nozawa, K., Doihara, H., Keto, Y., Kaku, H., Yokoyama, T., and Itou, H. (2014) Effects of novel TRPA1 receptor agonist ASP7663 in models of drug-induced constipation and visceral pain. *Eur. J. Pharmacol.* **723,** 288–293
45. Weng, Y., Batista-Schepman, P. A., Barabas, M. E., Harris, E. Q., Dinsmore, T. B., Kossyreva, E. A., Foshage, A. M., Wang, M. H., Schwab, M. J., Wang, V. M., Stucky, C. L., and Story, G. M. (2012) Prostaglandin metabolite induces inhibition of TRPA1 and channel-dependent nociception. *Mol. Pain.* **8,** 75
46. Materazzi, S., Benemei, S., Fusi, C., Gualdani, R., De Siena, G., Vastani, N., Andersson, D. A., Trevisan, G., Moncelli, M. R., Wei, X., Dussor, G., Pollastro, F., Patacchini, R., Appendino, G., Geppetti, P., and Nassini, R. (2013) Parthenolide inhibits nociception and neurogenic vasodilatation in the trigeminovascular system by targeting the TRPA1 channel. *Pain* **154,** 2750–2758
47. Andersson, D. A., Gentry, C., Moss, S., and Bevan, S. (2008) Transient receptor potential A1 is a sensory receptor for multiple products of oxidative stress. *J. Neurosci.* **28,** 2485–2494
48. Takahashi, N., Mizuno, Y., Kozai, D., Yamamoto, S., Kiyonaka, S., Shibata, T., Uchida, K., and Mori, Y. (2008) Molecular characterization of TRPA1 channel activation by cysteine-reactive inflammatory mediators. *Channels* **2,** 287–298
49. Andersson, D. A., Gentry, C., and Bevan, S. (2012) TRPA1 has a key role in the somatic pro-nociceptive actions of hydrogen sulfide. *PLoS ONE* **7,** e46917
50. Eberhardt, M., Dux, M., Namer, B., Miljkovic, J., Cordasic, N., Will, C., Kichko, T. I., de la Roche, J., Fischer, M., Suárez, S. A., Bikiel, D., Dorsch, K., Leffler, A., Babes, A., Lampert, A., *et al.* (2014) H2S and NO cooperatively regulate vascular tone by activating a neuroendocrine HNO-TRPA1-CGRP signalling pathway. *Nat. Commun.* **5,** 4381
51. Lennertz, R. C., Kossyreva, E. A., Smith, A. K., and Stucky, C. L. (2012) TRPA1 mediates mechanical sensitization in nociceptors during inflammation. *PLoS ONE* **7,** e43597
52. da Costa, D. S., Meotti, F. C., Andrade, E. L., Leal, P. C., Motta, E. M., and Calixto, J. B. (2010) The involvement of the transient receptor potential A1 (TRPA1) in the maintenance of mechanical and cold hyperalgesia in persistent inflammation. *Pain* **148,** 431–437
53. Ruparel, N. B., Patwardhan, A. M., Akopian, A. N., and Hargreaves, K. M. (2008) Homologous and heterologous desensitization of capsaicin and mustard oil responses utilize different cellular pathways in nociceptors. *Pain* **135,** 271–279
54. Gui, J., Liu, B., Cao, G., Lipchik, A. M., Perez, M., Dekan, Z., Mobli, M., Daly, N. L., Alewood, P. F., Parker, L. L., King, G. F., Zhou, Y., Jordt, S. E., and Nitabach, M. N. (2014) A tarantula-venom peptide antagonizes the TRPA1 nociceptor ion channel by binding to the S1-S4 gating domain. *Curr. Biol.* **24,** 473–483
55. Utkina, L. L., Andreev, Y. A., Rogozhin, E. A., Korostyleva, T. V., Slavokhotova, A. A., Oparin, P. B., Vassilevski, A. A., Grishin, E. V., Egorov, T. A., and Odintsova, T. I. (2013) Genes encoding 4-Cys antimicrobial peptides in wheat *Triticum kiharae* Dorof. et Migush.: multimodular structural organization, instraspecific variability, distribution and role in defense. *FEBS J.* **280,** 3594–3608
56. Honma, T., Hasegawa, Y., Ishida, M., Nagai, H., Nagashima, Y., and Shiomi, K. (2005) Isolation and molecular cloning of novel peptide toxins from the sea anemone *Antheopsis maculata*. *Toxicon* **45,** 33–41
57. Paulsen, C. E., Armache, J. P., Gao, Y., Cheng, Y., and Julius, D. (2015) Structure of the TRPA1 ion channel suggests regulatory mechanisms. *Nature* **520,** 511–517
58. Shelukhina, I., Paddenberg, R., Kummer, W., and Tsetlin, V. (2015) Functional expression and axonal transport of α7 nAChRs by peptidergic nociceptors of rat dorsal root ganglion. *Brain Struct. Funct.* **220,** 1885–1899
59. Raisinghani, M., Zhong, L., Jeffry, J. A., Bishnoi, M., Pabbidi, R. M., Pimentel, F., Cao, D. S., Evans, M. S., and Premkumar, L. S. (2011) Activation characteristics of transient receptor potential ankyrin 1 and its role in nociception. *Am. J. Physiol. Cell Physiol.* **301,** C587–C600
60. Altschul, S. F., Madden, T. L., Schäffer, A. A., Zhang, J., Zhang, Z., Miller, W., and Lipman, D. J. (1997) Gapped BLAST and PSI-BLAST: a new generation of protein database search programs. *Nucleic Acids Res.* **25,** 3389–3402
61. Kozlov, S., and Grishin, E. (2011) The mining of toxin-like polypeptides from EST database by single residue distribution analysis. *BMC Genomics* **12,** 88
62. Kozlov, S., and Grishin, E. (2005) Classification of spider neurotoxins using structural motifs by primary structure features. Single residue distribution analysis and pattern analysis techniques. *Toxicon* **46,** 672–686